Ab Initio QM/MM Modeling of the Hydroxylation Step in *p*-Hydroxybenzoate Hydroxylase

Lars Ridder,*,†,‡ Jeremy N. Harvey,† Ivonne M. C. M. Rietjens,§ Jacques Vervoort,|| and Adrian J. Mulholland*,†

School of Chemistry, University of Bristol, Bristol BS8 1TS, United Kingdom, Division of Toxicology, Wageningen University, Tuinlaan 5, 6703 HE Wageningen, The Netherlands, and Laboratory of Biochemistry, Wageningen University, Dreijenlaan 3, 6703 HA Wageningen, The Netherlands

Received: May 31, 2002; In Final Form: October 24, 2002

p-Hydroxybenzoate hydroxylase (PHBH) is the model enzyme for the microbial flavin-dependent monooxygenases. The aromatic hydroxylation of *p*-hydroxybenzoate by the reactive C4a-hydroperoxyflavin cofactor intermediate in PHBH has been studied by a combined ab initio quantum mechanics and molecular mechanics (QM/MM) method. Starting from a model of the C4a-hydroperoxyflavin intermediate in the PHBH reaction cycle, built on the basis of the crystal structure of the enzyme−substrate complex, a pathway for the hydroxylation step was calculated by imposing a reaction coordinate involving cleavage of the peroxide oxygen−oxygen bond and bond formation between the C3 atom of the substrate and the distal oxygen of the peroxide moiety of the cofactor. A QM/MM potential was used in which the QM region (49 atoms) was treated at the ab initio HF level with the 3-21G(d) or 6-31G(d) basis sets. The accuracy of various aspects of the QM/MM method for this system has been tested by comparison to higher-level calculations. Inclusion of electron correlation, applied here as B3LYP/6-311+G(d,p) and LMP2/6-31+G(d) single point energy corrections to the ab initio QM/MM structures, is shown to be essential to obtain barriers in agreement with the experimental rate constant. The calculated pathways support electrophilic aromatic substitution as the mechanism of this rate-limiting step in the PHBH catalyzed reaction cycle. The polarization of the QM region by the enzyme has been investigated. A potentially important catalytic interaction between the reacting OH group in the transition state (formally OH^+) and the backbone carbonyl of the Pro293 residue is identified from the calculations and is analyzed in detail. This interaction is calculated to lower the barrier by a catalytically significant 2−3 kcal/mol, corresponding to a 100-fold rate enhancement.

Introduction

There is great current interest in biological oxygenation reactions, in particular in elucidating the mechanisms of enzymes involved in oxygen activation and transfer,[1] both from the point of view of understanding the basic chemistry involved, and with a view to practical applications of such biocatalysts. One important family of oxygenase enzymes is that of the flavin-dependent monooxygenases. *p*-Hydroxybenzoate hydroxylase (PHBH) is an extensively studied representative of the flavin-dependent monooxygenase family. It catalyzes the hydroxylation of *p*-hydroxybenzoate at the ortho position with respect to the hydroxyl group, which is a crucial step in the biodegradation of a wide variety of aromatic compounds including lignin, a major component of wood and one of the most abundant biopolymers.

The reaction cycle of PHBH involves binding of the substrate, a two-electron reduction of the flavin cofactor by NADPH, and the incorporation of molecular oxygen to form the reactive C4a-peroxyflavin species. The mechanism by which this peroxyflavin intermediate hydroxylates the substrate is a key issue in the study of PHBH. Among the proposed reaction mechanisms are dioxygen transfer to the substrate,[2,3] homolytic cleavage of the peroxide bond[4−6] and a mechanism that proceeds via an open ring form of the flavin.[7,8] Several recent studies,[9−11] however, have supported an electrophilic aromatic substitution mechanism, which proceeds by heterolytic cleavage of the peroxide bond and results in the formation of a deprotonated C4a-hydroxyflavin intermediate of the cofactor and a hydroxycyclohexadienone intermediate (Figure 1). This hydroxycyclohexadienone is thought to convert nonenzymatically to catechol via keto−enol tautomerisation.

The precise mechanism of hydroxylation has remained uncertain for a long time. This is partly due to the short lifetime of the intermediate involved in this step, which has hampered its experimental identification. This is a typical problem in studies of enzyme-catalyzed reactions. It is often difficult to distinguish between alternative proposed mechanisms and to identify the reaction intermediates involved. Similarly, detecting and analyzing important interactions within the enzyme, for example interactions present only transiently during the reaction, is a formidable challenge even when good, relevant, structural data are available. In all these respects, mechanistic calculations and modeling of enzyme-catalyzed reaction mechanisms have an important role to play.[1] Combined quantum mechanics/molecular mechanics (QM/MM) methods are an increasingly important computational tool in this field.[12] They allow potentially accurate (but computationally expensive) QM treatment of the reacting part of the structure, while the interactions with

* Corresponding authors. L.R.: tel, +31 412 661924; e-mail, lars.ridder@organon.com. A.J.M.: tel, +44 117 928 9097; e-mail, adrian.mulholland@bristol.ac.uk.

† University of Bristol.

‡ Current address: Molecular Design & Informatics, N.V. Organon, P.O. Box 20, 5430 BH Oss, The Netherlands. Tel: +31 412 661924. E-mail: lars.ridder@organon.com.

§ Division of Toxicology, Wageningen University.

|| Laboratory of Biochemistry, Wageningen University.

10.1021/jp026213n CCC: $25.00
Published on Web 02/08/2003

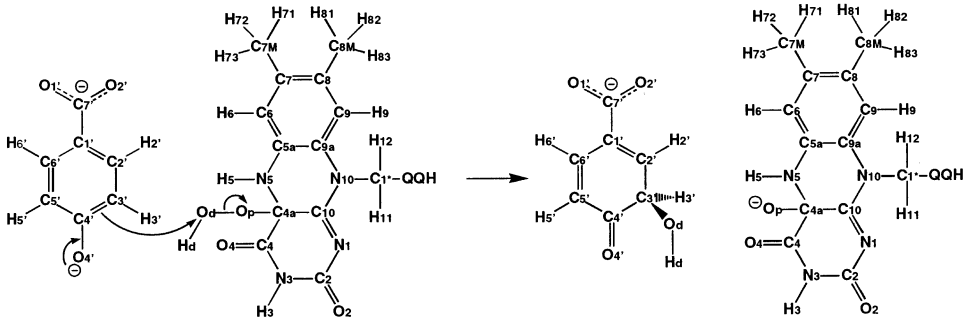

Figure 1. Modeled hydroxylation step in PHBH, according to an electrophilic aromatic substitution mechanism.

the surrounding enzyme are included, described at a computationally efficient MM level. An example of the utility of QM/MM investigations is provided by our earlier studies of the hydroxylation reaction in PHBH,[10,11,13] and in the mechanistically similar phenol hydroxylase.[13] These studies showed a correlation between calculated reaction barriers and overall experimental activation energies for a series of alternative substrates. The correlations supported the proposal of an electrophilic aromatic substitution mechanism[9] in which the substrate is activated by deprotonation.[7,14−16] They also identified the hydroxylation step as rate-limiting for the overall reaction at physiological pH. In addition, the calculations brought to light a number of important interactions, including the novel suggestion that a conserved proline residue specifically stabilizes the transition state of the reaction, thus catalyzing the hydroxylation step.

Many QM/MM applications on enzymes so far, including our previous studies on PHBH, have employed a semiempirical treatment of the QM region. Clearly, semiempirical methods are very useful in the context of large systems such as enzymes, as they often provide a reasonable accuracy at low computational costs. However, because of the approximations made in semiempirical molecular orbital theory and because these methods are parametrized on the basis of a broad but finite training set,[17,18] their accuracy should be tested and verified for the particular reaction mechanism under investigation. In principle, less approximate ab initio methods have the advantage of being more generally reliable and applicable. Ab initio QM/MM calculations are, however, extremely computationally demanding and have been carried out for relatively few enzyme reactions to date.[19−22] In the present study, ab initio QM/MM calculations are carried out on the hydroxylation step by PHBH, to investigate the mechanistic hypothesis of electrophilic aromatic substitution, and the roles of important active site interactions suggested by the earlier semiempirical QM/MM studies, at higher levels of QM theory. The performance of different levels of QM theory in QM and QM/MM calculations is tested. Results with differently sized basis sets are compared and the effect of electron correlation is investigated through hybrid density functional theory and local perturbation theory calculations. The results provide detailed insight into the rate-limiting step of this important model enzyme as well as into the achievements and limitations of the ab initio QM/MM method as compared to the semiempirical AM1 QM/MM model previously applied to study the enzyme.

Methods

A QM/MM model of the C4a-hydroperoxyflavin-substrate intermediate of PHBH was built, essentially as described previously,[11] on the basis of the crystal structure of oxidized PHBH in complex with the substrate *p*-hydroxybenzoate (PDB entry code 1PBE.PDB).[23,24] The substrate, modeled in its dianionic state,[7,11,16] and the C4a-hydroperoxyflavin ring of the cofactor[25,26] were described quantum mechanically, using a "link atom"[27] to allow the covalent bond between C1* and C2* of the cofactor ribityl chain to cross the QM-MM boundary. The QM region includes 49 atoms with overall charge −2e. The surrounding MM region (4841 atoms including all amino acid residues and 330 crystal water molecules) was described using the CHARMm 22 extended atom force field (in which only polar group hydrogens are modeled explicitly),[28] with no cutoff applied to nonbonded interactions. Hydrogen atoms on crystal water molecules were built using the HBUILD routine[29] in the CHARMM program. A 16 Å sphere around the center of the active site (chosen to be the distal oxygen of the peroxide moiety), including 1187 atoms, was optimized throughout the calculations, with all other atoms kept fixed. Extensive initial optimization of the model, to a gradient smaller than 0.01 kcal mol^{-1} $Å^{-1}$ (requiring 776 steps of Adopted Basis Newton−Raphson (ABNR) minimization), was performed by treating the QM region with the semiempirical AM1 method. Subsequent minimization and pathway calculations were performed using an ab initio HF/3-21G(d) treatment of the QM region. An approximate reaction coordinate, defined as the difference in length between the breaking peroxide bond and the forming substrate C3−cofactor distal oxygen bond, was scanned in steps of 0.3 Å. At each point along the reaction path, the 16 Å sphere around the center of the active site was relaxed by 25 steps of steepest descent (SD) minimization, followed by (up to 394 steps of) ABNR minimization until the RMS gradient dropped below 0.01 kcal mol^{-1} $Å^{-1}$. The last point on the path (r = 1.1 Å) was further minimized without reaction coordinate restraint to obtain the product structure of the reaction step. The pathway calculated this way required 2397 ab initio HF optimization steps, using 370 h of 32 processor parallel computer time (11840 h total unit processor time) on a Cray T3E−1200 supercomputer. The pathway thus obtained was refined by further minimizing the various points on the path, using the larger 6-31G(d) basis set in the QM region, until the RMS gradient dropped below 0.05 kcal mol^{-1} $Å^{-1}$. This required an additional 758 ab initio HF optimization steps using 500 h on 32 parallel processors (27 840 h total unit processor time).

The pathways thus obtained are compared to results obtained with a semiempirical QM/MM (AM1/CHARMM) treatment of the same model. In our previously described semiempirical QM/MM model[10,11] the optimization conditions applied were slightly different from those used in the present work. In the previous work a smaller sphere with a radius of 10 Å was optimized, the nonbonded interactions were subject to a nonbonded cutoff and a smaller step size of 0.1 Å was applied. To obtain an exact comparison between the semiempirical and ab initio QM/MM treatments, the semiempirical model was recalculated with the

conditions described above, i.e., a 16 Å sphere of optimized atoms and no nonbonded cutoff. The present and previous semiempirical QM/MM results are virtually identical. Comparison of energy profiles calculated with 0.1 and 0.3 Å steps along the reaction coordinate yielded identical energies, indicating that the larger step size used in the present study does not result in distorted pathways.

All QM/MM calculations were performed using CHARMM 27[30] interfaced to either MOPAC 4.0 (for semiempirical QM/MM calculations[27]) or GAMESS-US[31] (for ab initio QM/MM calculations[32]). The QM/MM interactions include electrostatic interactions, by accounting for the MM charges in the electronic Hamiltonian of the QM system, classical VDW terms as well as classical bonded terms to covalently link the QM and MM regions. The same QM/MM setup was used with both interfaces except for a difference in the implementation of the link atom. In the semiempirical calculations, the AM1 link atom does not "feel" the MM charges,[27] whereas the ab initio link atom does.[32,33] As the link atom is far away from the reacting atoms in the QM region, and the charges on the MM host group are set to zero, this difference is not expected to influence the relative energies in the calculations and therefore has no significant effect on the pathway results.

The Hartree−Fock method, used to describe the QM region, is a relatively low level of ab initio treatment. It does not include electron correlation, which is expected to be significant in the reaction studied here. On the other hand, even HF level ab initio QM/MM calculations already require a considerable computational effort. It was not feasible with the current implementation (which involves a full QM/MM calculation, with polarization of the QM region, SCF calculation, and calculation of forces at every geometry optimization step) to perform ab initio QM/MM at levels of QM treatment that do include electron correlation, even with the availability of supercomputer resources. Instead, we have investigated the importance of electron correlation by quantifying its effect in the gas phase and applying this as a correction to the QM/MM energies.[20] Such an approach is justified on the basis of a well-known phenomenon in quantum chemistry, that good geometries can be obtained at relatively low level of theory and using limited basis sets, whereas accurate energies require higher levels of theory and larger basis sets. For example, benchmark calculations on the so-called G2 molecule set[34] show that B3LYP/6-311+G(2d,p)//HF/3-21G(d) calculations (i.e., a single point B3LYP/6-311+G(2d,p) calculation performed on geometries optimized at the HF/3-21G(d) level) are almost as accurate as full B3LYP/6-311+G(2d,p) geometry optimizations.[35] In analogy to this procedure, we have applied single point B3LYP/6-311+G(d,p) and LMP2/6-31+G(d) calculations, implemented in Jaguar 4.1,[36] on the QM atoms in the gas phase, using the geometries optimized within the MM environment. Subsequently, the gas-phase energies at the higher level, relative to the gas-phase energy at the lower HF level, were applied as a correction to the QM/MM energies.

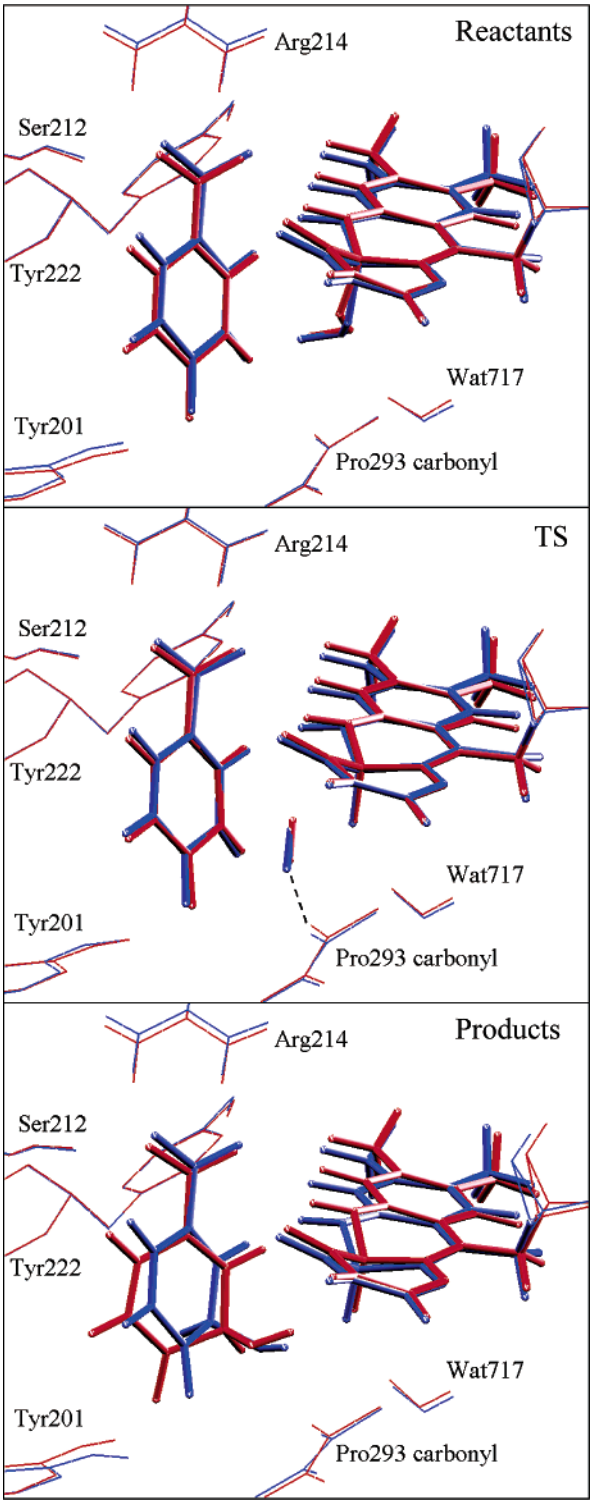

Figure 2. Comparison of structures obtained by semiempirical (AM1, blue) and ab initio (HF/6-31G(d), red) QM/MM pathway calculations, for the reactants, TS, and products of the hydroxylation step in PHBH. Solid bonds represent the QM region, whereas thin lines represent MM groups.

Results

Structural Comparison of Various QM/MM Models. Ab initio QM/MM reaction pathway calculations were performed using the HF/3-21G(d) and HF/6-31G(d) levels of theory. The geometries obtained along the reaction coordinate are very similar with both basis sets. (Coordinates of the QM atoms in the reactants, the transition state, i.e., at $r = -0.4$ Å, and the products of the QM/MM pathways at the different levels of QM treatment are given in the Supporting Information.) Figure 2 presents the ab initio QM/MM geometries obtained with the 6-31G(d) basis set, for three points along the reaction coordinate, in comparison with those obtained using semiempirical QM/MM. Along the reaction pathway, the distal OH group leaves the peroxy moiety of the C4a-hydroperoxyflavin cofactor and attaches to the aromatic C3 of *p*-hydroxybenzoate. This C3 carbon atom changes conformation from planar (sp^2) to tetrahedral (sp^3), while the C−C distances in the aromatic ring

TABLE 1: HF/6-31G(d) Mulliken Charges in Atomic Units of QM Atoms in the Reactant State ($r = -1.73$ Å), the Transition State (TS, $r = -0.4$ Å), and the Product State ($r = 1.23$ Å) of the QM/MM Pathway[a]

atom	reactants		TS		products	
C8	0.01	(0)	0.01	(0)	0.01	(0)
C8M	0.01	(6)	0.01	(6)	0.00	(6)
C9	−0.10	(1)	−0.10	(1)	−0.11	(0)
C9A	0.38	(0)	0.38	(0)	0.38	(0)
C5A	0.32	(−1)	0.31	(0)	0.33	(0)
C6	0.01	(−3)	0.01	(−4)	−0.05	(−3)
C7	0.00	(−1)	0.00	(−1)	0.01	(−1)
C7M	0.02	(3)	0.02	(3)	0.01	(3)
N10	−0.82	(0)	−0.82	(0)	−0.82	(0)
C10	0.79	(2)	0.77	(2)	0.78	(2)
C4A	0.36	(0)	0.39	(1)	0.41	(1)
N5	−0.90	(−1)	−0.88	(−2)	−0.90	(−1)
HN5	0.49	(−1)	0.46	(−1)	0.43	(−1)
N1	−0.81	(−5)	−0.82	(−5)	−0.84	(−5)
C2	0.98	(1)	0.97	(2)	0.97	(1)
O2	−0.66	(−3)	−0.68	(−3)	−0.70	(−3)
N3	−0.90	(−1)	−0.91	(−2)	−0.91	(−2)
HN	0.49	(8)	0.48	(8)	0.46	(7)
C4	0.86	(2)	0.86	(1)	0.84	(1)
O4	−0.61	(−7)	−0.62	(−6)	−0.66	(−6)
OP	−0.40	(−1)	−0.67	(−5)	−0.90	(−4)
OD	−0.50	(−2)	−0.35	(−1)	−0.82	(0)
HOD	0.53	(1)	0.53	(4)	0.54	(0)
C1′	−0.22	(−1)	−0.21	(−1)	−0.12	(0)
C7′	0.76	(0)	0.77	(1)	0.80	(1)
O1′	−0.85	(−8)	−0.85	(−7)	−0.82	(−7)
O2′	−0.86	(−4)	−0.85	(−5)	−0.82	(−5)
C2′	0.05	(1)	0.07	(1)	0.11	(0)
C6′	0.01	(1)	0.07	(2)	−0.02	(1)
C3′	−0.16	(8)	−0.13	(8)	−0.06	(9)
C5′	−0.31	(3)	−0.27	(3)	0.25	(2)
C4′	0.56	(1)	0.57	(1)	0.55	(0)
O4′	−0.86	(−4)	−0.85	(−3)	−0.63	(−1)
C1*	0.17	(0)	0.16	(0)	0.15	(0)
flavin	−0.14	(3)	−0.51	(−2)	−0.96	(0)
OH	0.02	(−1)	0.18	(3)	−0.28	(0)
substrate	−1.88	(−2)	−1.67	(−1)	−0.76	(0)

[a] Charges of aliphatic and aromatic hydrogen atoms have been included in the carbon atoms they are bound to. (The separate charges are available in the Supporting Information.) In parentheses are the effect of the protein (i.e., the given QM/MM charges minus charges from single point calculations in the gas phase, in hundredths of an atomic charge unit). Atom labels according to Figure 1.

change in line with formation of a cyclohexadienone ring. The distal OH group changes its hydrogen bonding arrangement twice. Initially, it accepts a hydrogen bond from a crystal water molecule (Wat717). Early in the reaction coordinate this hydrogen bond is lost, and instead the OH moiety then donates a hydrogen bond to the backbone carbonyl moiety of Pro293. In the final phase of the reaction pathway, this hydrogen bond is replaced by a hydrogen bond to the flavin proximal (hydroxylate) oxygen. Figure 2 reveals that with respect to atomic structure, very similar pathways are obtained with the ab initio and semiempirical QM/MM simulations. The main difference is observed in the product state. With ab initio QM/MM, a clear hydrogen bond is formed between the (new) hydroxyl group of the hydroxycyclohexadienone product and the hydroxylate oxygen of the C4a-hydroxyflavin (d(Hd−Op) = 1.65 Å, ∠(Od−Hd−Op) = 174.0°). This hydrogen bond is less clear with AM1 (d(Hd−Op) = 2.12 Å, ∠(Od−Hd−Op) = 159.1°). This difference could be due to AM1, which is known to often underestimate hydrogen bond strengths.[18,37]

Table 1 presents Mulliken atomic charges for the QM atoms at the HF/6-31G(d) level. The changes in geometry and the changes in Mulliken charges are in agreement with an electrophilic aromatic substitution mechanism, represented in Figure 1. Formally, OH^+ is transferred from the hydroperoxyflavin cofactor to the substrate. Indeed, the OH moiety is somewhat positively charged (+0.18) in the transition state, as compared to the reactant state (+0.02) and product state (−0.28) (Table 1). The changes in the charge on the substrate O4′ agree with its formal change from a charged hydroxylate oxygen to a neutral carbonyl oxygen. Also the change in charge on the distal oxygen Op of the cofactor is in line with the formation of the C4a-hydroxylate-flavin. Overall, a net negative charge of one electron moves from the substrate to the cofactor. Within the QM/MM implementation used, only Mulliken charges were available. The Mulliken population analysis has well-known limitations, such as the lack of convergence of the charges upon expanding the basis set.[38] For the QM atoms in the gase phase, using the HF/6-31* level of theory, the Mulliken charges were confirmed to be similar to charges derived from natural atomic orbital analysis (results provided in the Supporting Information),[39] which has some advantages over Mulliken analysis. This confirms that the Mulliken charges for the present system are satisfactory. The Mulliken atomic charges in Table 1 include the effect of polarization by the MM environment in the QM/MM model. To approximately quantify the effect of polarization, these charges from the QM/MM calculations were compared to charges obtained from single point calculations of the QM atoms in the gase phase. The differences between the charges in the QM/MM model and those in the gase phase represent the polarizing effect of the protein and are given in parentheses in Table 1.

Table 2 presents interatomic distances representing hydrogen bonds between the QM and MM regions for three points on the path and for the different levels of QM treatment. Most importantly, Table 2 shows that hydrogen bond interactions observed in the crystal structures of PHBH[24] and previously in the semiempirical QM/MM model[11] are maintained, with satisfactory geometries, in the ab initio QM/MM model. In particular, the transient stabilizing interaction of the Pro293 backbone carbonyl with the OH group in the transition state, previously identified in semiempirical QM/MM studies,[11,13] is also observed in the present ab initio QM/MM calculation. The results indicate that the ab initio QM/MM interactions are similar with the 3-21G(d) and 6-31G(d) basis sets. Generally, the ab initio QM/MM distances are shorter (by up to 0.2 Å) than with AM1 based QM/MM.

Comparison of Tables 1 and 2, provides insight in the stabilizing interactions between the QM and MM region. In particular, the Mulliken results clearly indicate the stabilizing effect of the protein on the negatively charged oxygens in the reactant dianionic *p*-hydroxybenzoate (O1′, O2′, and O4′) and the flavin-hydroxylate product (Op), presumably by the hydrogen bonds listed in Table 2. Also a transient polarizing effect of the protein surroundings on the OH group in the TS is evident, probably due to the above-mentioned interaction with the backbone carbonyl Pro293. Furthermore, the N1, O2, H3, and O4 atoms of the flavin ring are involved in hydrogen bonds to the protein backbone. The stabilizing effects of these hydrogen bonds are apparent from significant changes in the charges on these flavin atoms.

Energy Profiles along the Reaction Coordinate. Figure 3 presents the QM/MM energy profiles obtained with the QM region treated at the HF/3-21G(d), HF/6-31G(d), and AM1 levels, respectively. The profiles obtained with ab initio HF treatment of the QM atoms are comparable for the two basis sets, the main difference being a larger overall change in energy on reaction for the larger basis set. The energy barriers are

TABLE 2: QM/MM Distances from Optimized Models with the HF/3-21G(d), HF/6-31G(d), and AM1 Methods Used for the QM System, Representing Important Hydrogen Bond Interactions in the Active Site[a]

hydrogen bonds MM—QM (Å)	reactants			$r = -0.4$ Å			products		
	3-21G(d)	6-31G(d)	AM1	3-21G(d)	6-31G(d)	AM1	3-21G(d)	6-31G(d)	AM1
Ser212—OH···O1′	1.89	1.87	1.97	1.87	1.86	1.95	1.86	1.85	1.95
Arg214—NH1···O1′	1.87	1.77	1.85	1.73	1.74	1.83	1.75	1.75	1.81
Arg214—NH2···O2′	1.91	1.85	1.98	1.86	1.84	1.97	1.85	1.82	1.95
Tyr222—OH···O2′	1.92	1.87	1.96	1.84	1.83	1.93	1.89	1.88	1.95
Tyr201—OH···O4′	1.78	1.79	1.92	1.81	1.80	1.94	1.81	1.82	2.15
Pro293═O···Hd	2.40	2.38	2.44	1.82	1.83	1.93	2.67	2.62	2.31
Wat717—OH···Op	2.41	2.45	2.21	1.90	1.93	1.99	1.93	1.94	2.01
Wat717—OH···Od	1.94	1.94	2.07	2.99	2.94	2.93	3.40	3.43	3.81
Leu299—NH···N1	2.02	2.01	2.07	2.01	2.00	2.06	2.02	2.00	2.07
Asn300—NH···O2	1.98	1.97	1.96	1.95	1.95	1.94	1.97	1.96	1.97
Val47═O···H3	1.92	1.92	2.06	1.97	1.97	2.15	2.05	2.07	2.24
Val47—NH···O4	1.99	2.02	2.05	1.99	2.01	2.01	1.97	1.98	2.04
Gly46—NH···O4	1.84	1.87	1.93	1.89	1.93	1.95	1.89	1.93	1.95

[a] The structure at $r = -0.4$ Å represents the approximate transition state.

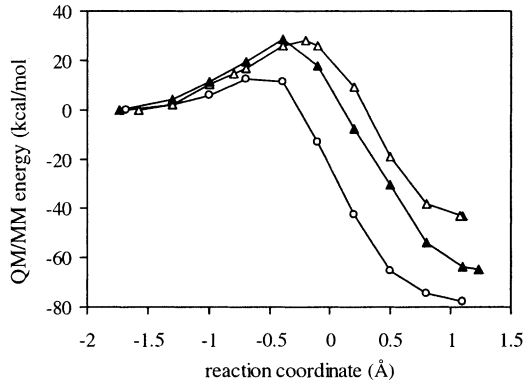

Figure 3. QM/MM energy profiles for the hydroxylation step, calculated with AM1 (open circles), HF/3-21G(d) (open triangles), and HF/6-31G(d) (solid triangles) level treatments of the QM region.

similar in height, about 30 kcal/mol, whereas the peaks in the two profiles are located at slightly different points on the reaction coordinate. To verify if these peaks, at $r = -0.2$ Å and $r = -0.4$ Å, respectively, are representative for the transition states on the reaction pathways at both levels, normal-mode analysis (using Jaguar 4.1) was performed on the isolated QM atoms of the corresponding structures. In both calculations, a large negative eigenvalue was obtained for the vibration that corresponds to the reaction process. In each case two additional (small) negative eigenvalues were obtained that corresponded to vibrations caused by the absence of the MM environment in the normal-mode analysis. (These "artificial" vibrations are a rotation of the methyl group C1*, which is covalently linked to the MM system in the full QM/MM model and a relative reorientation of the substrate and the flavin ring.) This result indicates that the maxima in the energy profiles are indeed reasonably close to the actual transition states of the model system. The slight variation in the predicted location of the transition state could be related to the calculated exothermicity by a simple Marcus relationship.

In terms of a Marcus relation[40] (between the exothermicity of the reaction and the height and location of the barrier), the earlier transition state with the 6-31G(d) basis set (compared to 3-21G(d)) is in line with the greater exothermicity at the higher level. The fact that the height of the barrier has not decreased would indicate that the so-called intrinsic barrier is somewhat higher with the 6-31G(d) basis set compared to that with 3-21G(d). The energy barriers are clearly overestimated at the HF level, in comparison to the experimental value of about 12 kcal/mol,[41] and calculations at higher QM levels (see below). The ab initio QM/MM barriers are also larger than the energy barrier obtained with the semiempirical (AM1) QM/MM method.[10,11]

Effect of Electron Correlation. To investigate the influence of the level of QM theory used in the modeling of the hydroxylation reaction, single point energies were calculated for the isolated QM atoms (i.e., in the gas phase) with various ab initio methods. The single point energies were calculated at the HF/3-21G(d) or HF/6-31G(d), B3LYP/6-311+G(d,p), and LMP2/6-31+G(d) levels of theory, using the QM geometries of the two ab initio QM/MM pathways with the 3-21G(d) and 6-31G(d) basis sets, respectively. The energy profiles thus obtained for each of the two ab initio QM/MM pathways are presented in Figure 4a,b and compared to results obtained in a similar way with AM1 (i.e., single point AM1 energies, in the gase phase, for QM parts of AM1/MM derived geometries). The barriers at the B3LYP/6-311+G(d,p) and LMP2/6-31+G(d) levels are significantly lower than the barriers obtained at the HF/3-21G(d) and HF/6-31G(d) levels. This indicates that inclusion of electron correlation is very important to obtain accurate ab initio energies for the hydroxylation reaction in PHBH. As the exothermicity of the reaction is not dramatically changed, it seems that, in terms of Marcus theory,[40] electron correlation lowers the intrinsic barrier of the reaction. Comparison of Figure 4a,b provides some insight into the sensitivity of the higher-level single point energies to the geometries used. The B3LYP/6-311+G(d,p) profiles are similar when geometries from the two QM/MM pathways are used, with the 3-21G(d) or 6-31G(d) basis sets: the barriers are 13.2 and 12.1 kcal/mol, respectively, and the maximum energies are found at the same point on the reaction coordinate, $r = -0.7$ Å. The LMP2/6-31+G(d) energies are more sensitive toward the geometries used: the barriers are 18.1 and 11.2 kcal/mol, at $r = -0.4$ Å and $r = -0.7$ Å, when geometries based on the 3-21G(d) and 6-31G(d) basis sets are used, respectively. The barriers obtained at the higher levels, especially with the geometries based on the 6-31G(d) basis set, are also in better agreement with the experimental value of about 12 kcal/mol.[41] Although these barriers (calculated in the gase phase, but using geometries from the reaction in the protein) could strictly not be compared with the experimental barrier for the reaction in the enzyme, it appears to be not unreasonable in this specific case, because the electrostratic effect of the protein (i.e., of the QM/MM electrostratic interactions) on the barrier for this step is found to be small.[11] The overall energy change on reaction, consistently about −55 kcal/mol for the correlated methods, seems relatively large. Unfortunately, no experimental data are available here for comparison. The results should not be used to draw detailed

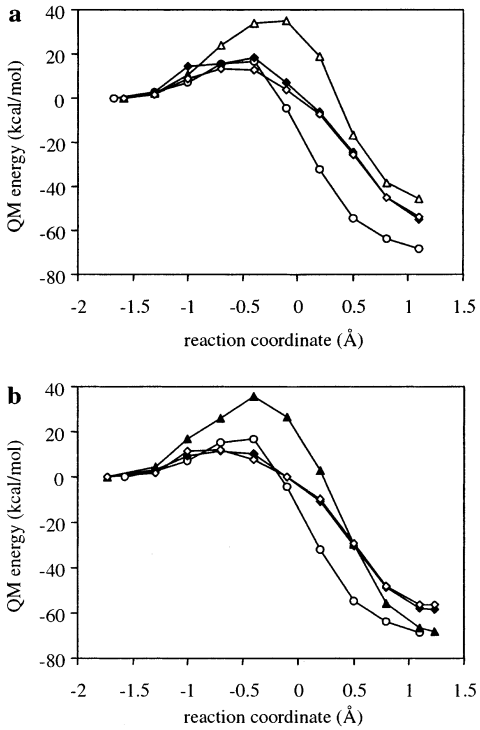

Figure 4. Gas-phase energy profiles obtained from single point calculations of the QM atoms at the HF (triangles), B3LYP/6-311+G(d,p) (open diamonds), and LMP2/6-31+G(d) (solid diamonds) levels, based on ab initio QM/MM geometries obtained with the (a) 3-21G(d) and (b) 6-31G(d) basis sets. AM1 energies (open circles) are based on AM1/MM geometries.

conclusions on the curvature of the higher-level energy profiles along the reaction coordinate, as the minimum energy pathways at the higher levels might have shown different behavior along the approximate reaction coordinate that was applied here at the HF level. Nevertheless, the profiles suggest that the TS occurs earlier on the reaction coordinate with the higher-level treatments including electron correlation. Comparison of the AM1 gas phase results with the various ab initio profiles suggests that although the overall shape of the profile is similar to the HF profiles, the barrier is much closer to those at the higher levels including electron correlation. Also, the position of the TS is somewhat earlier on the reaction coordinate, in better agreement with the higher level profiles. The difference between the gas-phase barriers for AM1 (16.5 kcal.mol) and those for B3LYP/6-311+G(d,p)//HF/6-31G(d) (12.1 kcal/mol) and LMP2/6-31+G(d)//HF/6-31G(d) (11.2 kcal/mol) is consistent with the previous finding that the QM/MM model with AM1 overestimates the barrier by approximately 5 kcal/mol.[10,11]

Subsequently, the difference between the gas-phase HF/6-31G(d) energies and the single point energies at the higher levels was applied as a correction to the ab initio QM/MM profile (with the 6-31G(d) basis set). In Figure 5, the resulting corrected profiles are compared to the ab initio HF/MM and AM1/MM profiles. The profiles corrected on the basis of LMP2/6-31+G(d) and B3LYP/6-311+G(d,p) have barriers of 5 and 6 kcal/mol, respectively. These barriers are too low in comparison to the experimental barrier of 12 kcal/mol.[41] It is important to note that in the corrected energies the QM/MM polarization and interaction energies are still represented at the lower HF/6-31G(d) level. The following section will show that the stabilization of the transition state by the protein is overestimated at this level of QM/MM treatment, explaining at least in part the low barriers of the corrected profiles.

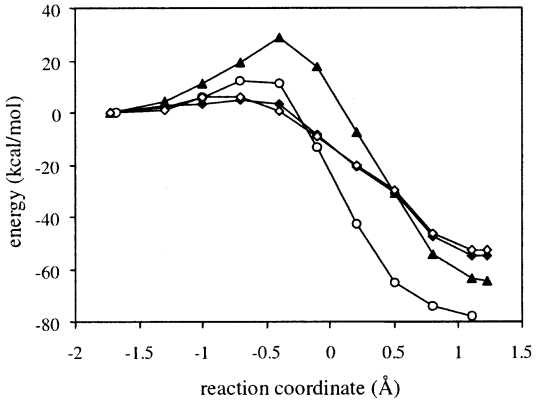

Figure 5. B3LYP/6-311+G(d,p) (open diamonds) and LMP2/6-31+G(d) (solid diamands) corrected QM/MM energy profiles (see text) compared to the ab initio (HF/6-31G(d), solid triangles) and semiempirical (AM1, open circles) QM/MM energy profiles.

Catalytic Role of Pro293. The interaction of the transferring OH group with the backbone carbonyl of Pro293 has been described for the first time on the basis of the previous semiempirical QM/MM modeling and was argued to be of catalytic importance because of its specific stabilization of the transition state.[11,13] The present ab initio QM/MM models reproduce this specific interaction with the transition state (Table 2). As the geometry optimization along the ab initio QM/MM pathway was performed entirely at the ab initio HF level (e.g., no initial semiempirical minimization was used for any of the pathway intermediates, only for the reactants), this independently shows the formation of this interaction. Because the interaction appears to be of potential importance in the reaction, its effect (and of the protein as a whole) on the energetics of the reaction was further investigated through several additional calculations using the different structures along the pathway. These calculations also tested the accuracy of the QM/MM representation of this crucial interaction.

First, single point energies were calculated along the two ab initio QM/MM pathways in which all MM atoms were removed or in which the MM charges on the carbonyl atoms of only Pro293 were removed. Parts a and b of Figure 6 show, for each path respectively, two profiles presenting the relative differences in QM energies between the full QM/MM model and the two series of single point calculations. Thus, these curves represent stabilization profiles, indicating the effects of the whole protein, and of the backbone carbonyl hydrogen bond alone, respectively, on the energies along the reaction coordinate relative to the reactants. For both pathways, the two curves indicate a stabilization of the QM region around the transition state. The similarities in these curves indicate that the interaction with the Pro293 carbonyl makes a distinctive contribution to the stabilization profile in the protein. Clearly, many other interactions affect the relative energy along the path, such as hydrogen bonds with Wat717 and Tyr201, as shown previously by our semiempirical QM/MM calculations.[11] This previous work showed, for example, that the stabilizing effect of Tyr201 on O4′ of the substrate decreases as the reaction proceeds, in line with its change from a formal negatively charged hydroxylate oxygen to a formally neutral carbonyl oxygen and the lengthening of the hydrogen bond between Tyr201 and O4′, reported in Table 2. Similarly, the stabilizing effect of Wat717 on Op increases because this oxygen becomes formally negatively charged as the reaction proceeds, in line with the shortening of this hydrogen bond indicated in Table 2. Apparently, the total stabilizing effect of the QM/MM interactions, apart from the interaction with Pro293, is approximately constant along the

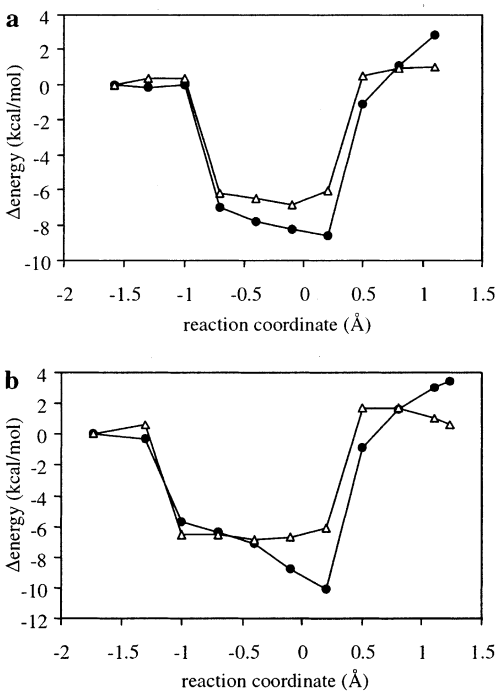

Figure 6. Stabilization profiles along the reaction coordinate representing the effect of the protein (solid circles), and of the backbone carbonyl of Pro293 only (open triangles), on the energy of the QM atoms treated at the (a) HF/3-21G(d) and (b) HF/6-31G(d) levels, relative to the reactants.

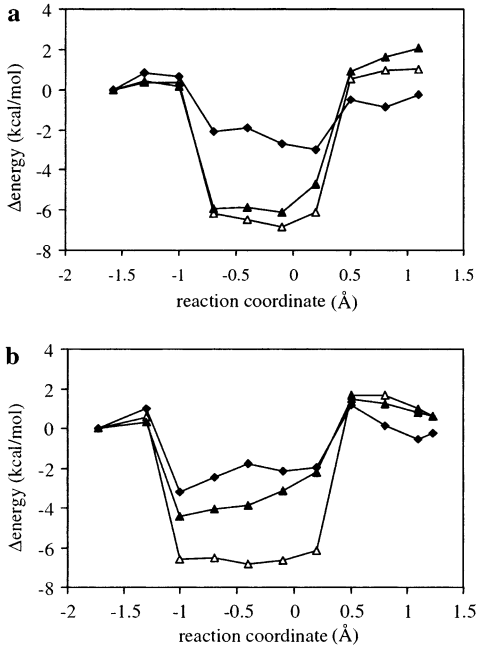

Figure 7. Stabilization of the QM atoms by the (MM) backbone carbonyl of Pro293 in the ab initio QM/MM model (open triangles) using (a) the 3-21G(d) and (b) 6-31G(d) basis sets, compared to full ab initio HF6-31G(d) (solid triangles) and B3LYP/6-311+G(d,p)//HF6-31G(d) (solid diamonds) calculations on models including formamide to represent the backbone carbonyl (see text for details).

path. In Figure 6a, a clear stabilization of 6−7 kcal/mol is observed for the -0.7 Å $\leq r \leq$ 0.2 Å region of the reaction pathway obtained with the 3-21G(d) basis set. This is exactly the region in which the QM/MM optimized geometries show a hydrogen bond interaction between the Pro293 carbonyl and the reacting OH group of the QM system. Comparison with Figure 6b indicates that for the HF/6-31G(d) based pathway a similar stabilization by the Pro293 carbonyl occurs, starting somewhat earlier on the reaction coordinate (at $r = -1.0$ Å) in agreement with the existence of the hydrogen bond.

The effect of the backbone carbonyl of Pro293 was further tested by full QM calculations on the reacting substrate and flavin atoms (i.e., the QM region of the QM/MM model) and a molecule of formamide representing the peptide bond between Pro293 and Thr294. Geometries for this model system were extracted from the QM/MM models, for all points on the pathways obtained with the two basis sets. In the model structures, the coordinates for the backbone atoms N_{Thr294}, C_{Pro293}, and O_{Pro293} were used to build a molecule of formamide by replacing bonds to adjacent backbone atoms by bound hydrogens. Partial geometry optimization of the resulting model structures was performed at the HF level (using the basis set of the corresponding QM/MM pathway) in which all but four atoms were frozen. These four optimized atoms consisted of the three hydrogen atoms of formamide and the hydrogen atom of the reacting OH group. The energy profiles obtained in this way yield barriers that are lower than for the energy profiles obtained from single point calculations on the isolated QM atoms (i.e., the QM atoms of the QM/MM model, not including formamide). The difference between the energy profiles with and without formamide represents the stabilizing effect of the backbone carbonyl along the reaction coordinate. Figure 7 compares the stabilization by formamide obtained from full QM calculations to the stabilization by the Pro293 backbone derived from the QM/MM model (as in Figure 6). The results indicate that at the HF/3-21G(d) level the QM/MM results for this interaction are consistent with full QM results (i.e., ∼6 kcal/mol) for the formamide model. At the HF/6-31G(d) level, however, the full QM model predicts a weaker interaction (∼4 kcal/mol) than the QM/MM model. Figure 7 also presents stabilization profiles obtained from single point B3LYP/6-311+G(d,p) calculations on the full QM models. Using these results as a reference, they indicate that the ab initio QM/MM models and the full ab initio HF formamide models overestimate the stabilization of the transition state by the backbone carbonyl. The results at the B3LYP/6-311+G(d,p) level indicate a stabilization of 2−3 kcal/mol.

Discussion

The hydroxylation step in PHBH is an excellent problem for investigation by QM/MM modeling and a good test case for the validation of new QM/MM methods. A high-resolution crystal structure of the enzyme with bound *substrate* (with cofactor in the oxidized form) is available,[23,24] which was a good starting point for calculations. The reactive C4a-hydroperoxyflavin intermediate is formed in the so-called "in" conformation, in which the active site is buried and shielded from bulk solvent, preventing unproductive wastage of the hydroperoxyflavin intermediate. In this intermediate state, the substrate and the reactive C4a-hydroperoxyflavin are tightly oriented by the enzyme environment. This can be modeled adequately by a QM/MM approach in which a molecular mechanical region describing the enzyme surrounds the quantum mechanically treated reacting species. The highly structured active site can be properly represented by a single conformation, and therefore an adiabatic mapping approach to modeling the reaction is suitable. This has been directly demonstrated for PHBH by the correlation between experimental barriers and those calculated by adiabatic mapping in earlier, semiempirical QM/MM studies.[10,13] Thus, the computationally expedient procedure of minimization along an approximate reaction pathway can be followed with confidence in this case (in contrast to solvent-exposed or conforma-

tionally variable active sites, which require better sampling of relevant enzyme−substrate conformations and solvent configuration[42]).

A primary practical consideration in ab initio QM/MM modeling is the amount of computer time required for these calculations. In the QM/MM implementation applied,[27,32] the atomic charges of the MM atoms are included directly in the QM one-electron Hamiltonian, and the atoms in the immediate MM environment as well as the QM atoms are allowed to move at every optimization step. This flexibility allows realistic adjustment of the (MM) protein environment to the electronic changes along the reaction pathway, effects that are potentially highly significant. Together with the large size of the QM system to be treated in the present model, this required a considerable computational effort.

The GAMESS-US/CHARMM implementation has so far not been used as widely as semiempirical QM/MM methods. The present study provides a test of this ab initio QM/MM method, as well as a verification of mechanistic conclusions from earlier semiempirical studies. The ab initio Hartree−Fock method, by neglecting electron correlation, generally overestimates activation barriers. In the present case of the hydroxylation step, this overestimation appears to be particularly significant. The observed barrier of 30 kcal/mol is about 2.5 times higher than the experimental barrier (12 kcal/mol[41]). The gas-phase single point energies at higher levels of theory including electron correlation indeed show dramatically lower energy barriers, which are much closer to the experimental value. The agreement between the higher-level energy barriers and the experimental value, together with the previously reported linear correlation between the calculated QM/MM barriers and the logarithm of the experimental rate constants,[10] strongly supports the modeled electrophilic aromatic substitution as the mechanism of the rate-limiting hydroxylation step.

It is clear that AM1, although it does not include electron correlation explicitly, provides a barrier that is much closer to the higher-level result than the ab initio HF method. This illustrates a well-known feature of semiempirical methods: instead of including computationally expensive terms (such as electron correlation) explicitly, it accounts for these terms implicitly through its parametrization to reproduce experimental data. The reaction studied here involves cleavage of the hydroperoxide bond of the complex C4a-hydroperoxyflavin species, which is a challenging system from a computational point of view. The present results indicate that AM1 gives a reasonably accurate result for this reaction pathway.

Nevertheless, the ab initio QM/MM results provide important supporting information with respect to the geometries along the reaction coordinate. It is useful to mention that applying B3LYP/6-311+G(d,p) single point energies on the QM geometries obtained from the AM1 based QM/MM pathways (results not shown) does not result in a smooth "continuous" profile as with the ab initio HF geometries. Thus, the ab initio HF geometries appear to be in better agreement with the higher-level methods than those from AM1. This probably concerns mainly the bond lengths in the AM1 and ab initio HF optimized structures, as the overall geometries (i.e., angles and dihedral angles) along the ab initio QM/MM pathway are very similar to those obtained by semiempirical QM/MM.

When single point energies at the higher levels are used to correct the QM/MM profiles, the barrier to the hydroxylation reaction is underestimated. A small error could be expected to come from the LMP2/6-31+G(d) and B3LYP/6-311+G(d,p) energies, as they were calculated on the basis of lower level geometries and because the LMP2 and B3LYP methods are known to sometimes underestimate barriers. However, a more important source for the underestimated barrier in the corrected profiles may be due to a limitation of the QM/MM interactions, which are still included at the lower HF/6-31G*/MM level. At this level, the stabilization of the transition state by the enzyme is approximately 6−7 kcal/mol (Figure 6). By comparison to B3LYP/6-311+G(d,p) treatment of the key interaction between the transferring OH group in the transition state and the Pro293 backbone carbonyl, the stabilization of the transition state seems to be overestimated by about 4 kcal/mol by the ab initio (HF) QM/MM method. The catalytic effect of the protein on the hydroxylation step, therefore, can be estimated to be on the order of 2 kcal/mol (in addition to this, the fact that the active site is preorganized to stabilize the transition state will assist catalysis[43]). This is a relatively small effect, which reflects the idea that the main role of the enzyme is to bring the cofactor and substrate together in their activated forms, i.e., the C4a-hydroperoxy form of the cofactor and the dianionic form of the substrate.[11] The hydroxylation step itself, subsequently, requires little catalysis, i.e., mainly by the interaction with the backbone carbonyl.

The QM/MM distances representing hydrogen bond interactions in the present model are generally shorter with ab initio HF than with AM1 (Table 2). This may indicate that the QM/MM nonbonded interactions are stronger using ab initio HF, a possibility supported by the present analysis of the transient hydrogen bond interaction of the transferring OH group with the Pro293 backbone carbonyl. The present observations are consistent with a study by Lyne et al., who compared the same methods for the water dimer and the water−chloride complex.[44] Their results for these two complexes indicate that, at the HF/6-31G(d) level, the QM/MM interaction energies are overestimated relative to full QM (by 1.5 kcal/mol for $(H_2O)_2$) and experimental results (by 2 kcal/mol for $(H_2O)_2$), whereas with AM1, the QM/MM interactions are underestimated relative to experiment (by 1−2 kcal/mol).

Because the same classical VDW parameters were used in the semiempirical and ab initio QM/MM interactions, the differences in the QM/MM interactions described above are entirely due to a difference in the electrostatic interactions. It is useful to note that the electrostatic interactions are implemented differently in the semiempirical and ab initio QM/MM methods. In ab initio QM/MM, the MM atoms are included as point charges in the electronic Hamiltonian and the interactions with the QM nuclei are calculated by a Coulomb term.[44] In MNDO type methods (like AM1), only valence electrons are treated explicitly, whereas the inner electrons are combined with the nucleus into a positive core. In the MNDO core−core repulsion and core−electron attraction terms, the monopole charge distribution of the atomic core is represented by an s orbital. This core−core repulsion term requires further corrections by exponential and Gaussian (AM1) functions of the interatomic distance.[17,18] In the development of semiempirical QM/MM, it was found to be a good approach to treat the MM atoms as (modified) MNDO type cores in the QM Hamiltonian.[27] Interestingly, the semiempirical QM/MM hydrogen bond interactions are often better than full semiempirical QM treatment,[27,42] which has well-known limitations in describing these interactions.[18,37] Ab initio HF is much better at describing hydrogen bonds than AM1, and an interesting question is whether it also provides more accurate results in QM/MM interactions.

Although a comprehensive test of the nonbonded interactions between the QM and MM regions was beyond the scope of the

present study, one important interaction has been selected for a detailed analysis. On the basis of our previous semiempirical QM/MM modeling of the hydroxylation reaction,[11] we suggested the backbone carbonyl moiety of Pro293 to be involved in a very unusual interaction, one that is specific to the transition state, and therefore purely catalytic in nature. This suggestion is reinforced by the present results from ab initio QM/MM modeling. The stabilization of the transition state by this interaction was previously estimated to be on the order of 3 kcal/mol on the basis of an amino acid decomposition analysis of the semiempirical QM/MM model.[11] Analysis of the present ab initio QM/MM model yields an estimate of about 6 kcal/mol. This interaction, however, is shown to be overestimated by the ab initio HF/MM potential in comparison with full B3LYP/6-311+G(d,p) energies for this interaction. The latter suggest a transition state stabilization of 2−3 kcal/mol, which is consistent with the previous estimate from the semiempirical QM/MM model[11] and corresponds to an increase in catalytic rate constant of about 2 orders of magnitude.

The backbone carbonyl involved in the catalytic interaction is part of a loop structure with a number of highly conserved residues. The proline at this position is part of the FAD fingerprint motif, which is characteristic of the family of flavin-dependent monooxygenases.[45,46] Previous QM/MM modeling of the homologous reaction step in another member of this family, phenol hydroxylase, has indicated that the backbone carbonyl of the conserved proline interacts likewise with the transferring OH group, which suggests a wider importance of this interaction for transition state stabilization in the family of flavin monooxygenases.[13] It was argued that a proline residue at this position could be favorable for restraining the backbone into an optimal conformation for the transition state stabilization.[13] Recently, the Pro293Ser mutant of PHBH was reported to exhibit a decreased rate of hydroxylation, theoretically corresponding to a destabilization of the hydroxylation transition state by 1.1 kcal/mol.[47] Although a backbone carbonyl is still present in this mutant, the backbone conformation and flexibility are influenced by the Pro293Ser mutation.[47] Because this is likely to affect the efficiency at which the transient interaction between the backbone carbonyl and the transition state of hydroxylation is formed, the reduced rate and efficiency of hydroxylation in the Pro293Ser mutant appears to confirm the catalytic importance of the interaction with the backbone carbonyl in the transition state, identified in our previous[11,13] and present QM/MM studies.

Acknowledgment. This research has been supported by a Marie Curie Fellowship of the European Community program Quality of Life within the Fifth Framework under contract number QLRI-CT-1999-51244. A.J.M. is an EPSRC Advanced Research Fellow.

Supporting Information Available: Tables of atomic charges from Mulliken analysis and Natural Atomic Orbital analysis. Coordinates of QM atoms of the reactants, TS (i.e., $r = -0.4$ Å) and products of the QM/MM pathways based on HF/3-21G(d), HF/6-31G(d), and AM1 treatment of the QM region. This material is available free of charge via the Internet at http://pubs.acs.org.

References and Notes

(1) Siegbahn, P. E. M.; Blomberg, M. R. A. *Chem. Rev.* **2000**, *100*, 421.
(2) Kemal, C.; Bruice, T. *J. Am. Chem. Soc.* **1979**, *101*, 1635.
(3) Keum, S. R.; Gregory, D. H.; Bruice, T. C. *J. Am. Chem. Soc.* **1990**, *112*, 2711.
(4) Anderson, R. F.; Patel, K. B.; Stratford, M. R. L. *J. Biol. Chem.* **1987**, *262*, 17475.
(5) Anderson, R. F.; Patel, K. B.; Vojnovic, B. *J. Biol. Chem.* **1991**, *266*, 13086.
(6) Peräkylä, M.; Pakkanen, T. A. *J. Am. Chem. Soc.* **1993**, *115*, 10958.
(7) Entsch, B.; Ballou, D. P.; Massey, V. *J. Biol. Chem.* **1976**, *251*, 2550.
(8) Husain, M.; Entsch, B.; Ballou, D. P.; Massey, V.; Chapman, J. P. *J. Biol. Chem.* **1980**, *255*, 4189.
(9) Maeda-Yorita, K.; Massey, V. *J. Biol. Chem.* **1993**, *268*, 4134.
(10) Ridder, L.; Mulholland, A. J.; Vervoort, J.; Rietjens, I. M. C. M. *J. Am. Chem. Soc.* **1998**, *120*, 7641.
(11) Ridder, L.; Mulholland, A. J.; Rietjens, I. M. C. M.; Vervoort, J. *J. Mol. Graphics Mod.* **1999**, *17*, 163.
(12) Mulholland, A. J. In *Theoretical Biochemistry − Processes and Properties of Biological Systems*; Theoretical and Computational Chemistry, Vol. 9; Erikkson, L. A., Ed.; Elsevier: Amsterdam, 2001
(13) Ridder, L.; Mulholland, A. J.; Rietjens, I. M. C. M.; Vervoort, J. *J. Am. Chem. Soc.* **2000**, *122*, 8728.
(14) Entsch, B.; Palfey, B. A.; Ballou, D. P.; Massey, V. *J. Biol. Chem.* **1991**, *266*, 17341.
(15) Eschrich, K.; Van Der Bolt, F. J. T.; De Kok, A.; Van Berkel, W. J. H. *Eur. J. Biochem.* **1993**, *216*, 137.
(16) Vervoort, J.; Rietjens, I. M. C. M.; Van Berkel, W. J. H.; Veeger, C. *J. Biochem.* **1992**, *206*, 479.
(17) Dewar, M. J. S.; Thiel, W. *J. Am. Chem. Soc.* **1977**, *99*, 4899.
(18) Dewar, M. J. S.; Zoebisch, E. G.; Healy, E. F.; Stewart, J. J. P. *J. Am. Chem. Soc.* **1985**, *107*, 3902.
(19) Harrison, M. J.; Burton, N. A.; Hillier, I. H. *J. Am. Chem. Soc.* **1997**, *119*, 12285.
(20) Mulholland, A. J.; Lyne, P. D.; Karplus, M. *J. Am. Chem. Soc.* **2000**, *122*, 534.
(21) Zhang, Y. K.; Liu, H. Y.; Yang, W. T. *J. Chem. Phys.* **2000**, *112*, 3483.
(22) Hayashi, S.; Ohmine, I. *J. Phys. Chem. B* **2000**, *104*, 10678−10691.
(23) Wierenga, R. K.; De Jong, R. J.; Kalk, K. H.; Hol, W. G. J.; Drenth, J. *J. Mol. Biol.* **1979**, *131*, 55.
(24) Schreuder, H. A.; Prick, P. A. J.; Wierenga, R. K.; Vriend, G.; Wilson, K. S.; Hol, W. G. J.; Drenth, J. *J. Mol. Biol.* **1989**, *208*, 679.
(25) Schreuder, H. A.; Hol, W. G. J.; Drenth, J. *Biochemistry* **1990**, *29*, 3101.
(26) Vervoort, J.; Müller, F.; Lee, J.; Moonen, C. T. W.; Van den Berg, W. A. M. *Biochemistry* **1986**, *25*, 8062.
(27) Field, M. J.; Bash, P. A.; Karplus, M. *J. Comput. Chem.* **1990**, *11*, 700.
(28) Quanta, Quanta, Molecular Simulations Inc., 200 Fifth Avenue, Waltham, MA., 1993
(29) Brunger, A. T.; Karplus, M. *Proteins* **1988**, *4*, 148.
(30) Brooks, B. R.; Bruccoleri, R. E.; Olafson, B. D.; States, D. J.; Swaminathan, S.; Karplus, M. *J. Comput. Chem.* **1983**, *4*, 187.
(31) Schmidt, M. W.; Baldridge, K. K.; Boatz, J. A.; Elbert, S. T.; Gordon, M. S.; Jensen, J. H.; Koseki, S.; Matsunaga, N.; Nguyen, K. A.; Su, S. J.; Windus, T. L.; Dupuis, M.; Montgomery, J. A. *J. Comput. Chem.* **1993**, *14*, 1347.
(32) Eurenius, K. P.; Chatfield, D. C.; Brooks, B. R.; Hodoscek, M. *Int. J. Quantum Chem.* **1996**, *60*, 1189.
(33) Reuter, N.; Dejaegere, A.; Maigret, B.; Karplus, M. *J. Phys. Chem. A* **2000**, *104*, 1720.
(34) Curtiss, L. A.; Raghavachari, K.; Trucks, G. W.; Pople, J. A. *J. Chem. Phys.* **1991**, *94*, 7221.
(35) Foresman, J. B.; Frisch, *Æ. Exploring chemistry with electronic structure methods*; Gaussian, Inc.: Pittsburgh, PA, 1996.
(36) Jaguar, Schrödinger, Inc., Portland, OR, 2000.
(37) Mulholland, A. J.; Richards, W. G. *J. Phys. Chem. B* **1998**, *102*, 6635.
(38) Jensen, F. *Introduction to Computational Chemistry*; John Wiley & Sons Ltd.: West Sussex, U.K., 1999.
(39) Glendening, E. D.; Badenhoop, J. K.; Reed, A. E.; Carpenter, J. E.; Weinhold, F. NBO 4.M; Theoretical Chemistry Institute, University of Wisconsin: Madison, 1999
(40) Marcus, R. A. *J. Phys. Chem.* **1968**, *72*, 891.
(41) Van Berkel, W. J. H.; Müller, F. *Eur. J. Biochem.* **1989**, *179*, 307.
(42) Ridder, L.; Rietjens, I. M. C. M.; Vervoort, J.; Mulholland, A. J. *J. Am. Chem. Soc.* **2002**, *124*, 9926
(43) Warshel, A. *Curr. Opin. Struct. Biol.* **1992**, *2*, 230.
(44) Lyne, P. D.; Hodoscek, M.; Karplus, M. *J. Phys. Chem.* A **1999**, *103*, 3462.
(45) Eppink, M. H.; Schreuder, H. A.; Van Berkel, W. J. H. *Protein Sci.* **1997**, *6*, 2454.
(46) Dimarco, A. A.; Averhoff, B. A.; Kim, E. E.; Ornston, L. N. *Gene* **1993**, *125*, 25.
(47) Palfey, B. A.; Basu, R.; Frederick, K. K.; Entsch, B.; Ballou, D. P. *Biochemistry* **2002**, *41*, 8438.